Ninth International Conference on
THIN-WALLED STRUCTURES – ICTWS2023
Sydney, Australia, Nov 29 – Dec 1, 2023

A NOVEL FUNCTIONAL FORM FOR THE APPLICATION OF THE DIRECT STRENGTH METHOD

Benjamin W. Schafer* and Robert S. Glauz**

* Johns Hopkins University
e-mail: schafer@jhu.edu

** RSG Software
e-mail: glauz@rsgsoftware.com

Keywords: Cold-Formed Steel Design; Direct Strength Method; Codes and Standards.

Abstract. *The objective of this paper is to summarize work to date on a novel functional form for the application of the Direct Strength Method in cold-formed steel design. The Direct Strength Method was first adopted in North America in 2004 and provided a means to use the local, distortional, and global elastic cross-section slenderness to predict the strength in bending and compression for thin-walled cold-formed steel members without recourse to effective width or element-by-element calculations. The method was subsequently extended to shear, combined actions, elevated temperatures, web crippling, and into other materials such as stainless steel and aluminum. The original functional form of the Direct Strength Method followed a variation of the effective width expression developed by George Winter; however, this expression provides only limited means to adjust the strength as a function of slenderness and must be spliced (or truncated) with other functions at low slenderness. Recently, a new simple continuous function in a fractional form with two coefficients has been developed by the authors and calibrated to the existing Direct Strength Method data. This simple expression provides a ready means to handle the shape of the strength transition at low and high slenderness – and to establish and vary the post-buckling strength. With this new functional form the authors provided a single solution for flexural members that handles local and distortional buckling including inelastic reserve up to plastic moment, unsymmetric sections and neutral axis shift, and members with holes. Utilizing the same form, similar advances were developed for compression members, members directly designed in combined bending and flexure, open sections in torsion, combined bending and torsion, and more. The paper provides a basic discussion of the continuous fractional form that is employed, how it is adjusted for various situations, and some of its limitations. Work of others utilizing this new form is also summarized. Numerous advances remain for generalized slenderness approaches such as the Direct Strength Method; the new recommended form provides a stable foundation for those efforts.*

1 INTRODUCTION

The design strength for local buckling of cold-formed steel members has utilized the Effective Width Method (EWM) for decades. The alternative Direct Strength Method (DSM) has been available in AISI S100 [1] since the 2004 edition, and in AS/NZS 4600 [2] since the 2005 edition. This method also includes strength expressions for distortional buckling.

Adoption of DSM for conventional shapes (C and Z sections) has increased in recent years, leading to validation of the method applied to other cold-formed steel members. A number of studies have shown some deficiencies in the DSM prediction for sections unsymmetric about the axis of bending. For example, Baur and LaBoube [3] and Nuttayasakul and Easterling [4] performed tests on the distortional buckling strength of complex hat shapes typically used as truss chord members, where DSM underpredicts the strength at low slenderness and overpredicts the strength at high slenderness. Further, Oey and Papangelis [5] evaluated a variety of C sections in minor axis bending with web in compression where DSM underpredicts the local buckling strength across all slenderness values. Studies on the strength of deck profiles by Raebel and Gwozdz [6] and Degtyarev [7] all show that opportunities for DSM improvement exists.

A recent study by Glauz and Schafer [8] proposed modifications to DSM to address the strength of these unsymmetrical sections in flexure, and further developed a new form of DSM equation that better reflects the flexural strength behavior unique to unsymmetric sections. This equation form provides further opportunities for simplifying DSM strength calculations beyond flexure. This paper summarizes the work of Glauz and Schafer [8] for flexural members, and presents an extension of the proposed equation form to compression members, members with holes, beam-columns, and shear strength.

2 FLEXURAL MEMBERS

The flexural tests supporting the current direct strength equations for local and distortional buckling consist primarily of C and Z sections bending about the major axis. Other tests for hat sections and trapezoidal deck were also evaluated, but tended to have more scatter associated with the level of asymmetry. Subsequent tests for C sections in minor axis bending showed even greater deviation from the current DSM equations.

For unsymmetric sections, two key factors alter the flexural strength: a) the shape factor $k_s=M_p/M_y$ is typically larger with asymmetry because first yield for M_y occurs at only one of the extreme fibers (tension or compression), and b) as slenderness increases, more stress redistribution occurs, sometimes favorable to the strength and sometimes unfavorable. Both of these factors can influence the strength curve throughout the range of slenderness, from inelastic reserve to post-buckling.

The local and distortional buckling equations proposed by Glauz and Schafer [8] for flexural members are:

$$\frac{M_{n\ell}}{k_s M_{ne}} = \frac{1+0.10\alpha_s\lambda_\ell^2}{1+0.55\beta_s\lambda_\ell^2} \qquad \lambda_\ell^2 = \frac{M_{ne}}{M_{cr\ell}} \tag{1}$$

$$\frac{M_{nd}}{M_p} = \frac{1+0.07\alpha_s\lambda_d^2}{1+0.60\beta_s\lambda_d^2} \qquad \lambda_d^2 = \frac{M_y}{M_{crd}} \tag{2}$$

where M_{ne} is the nominal lateral torsional buckling moment (not to exceed M_y), M_y is the yield moment, M_p is the plastic moment, $M_{cr\ell}$ is the critical elastic local buckling moment, M_{crd} is the critical elastic distortional buckling moment, λ_ℓ is the local buckling slenderness, and λ_d is the distortional buckling slenderness. The term β_s is the symmetry factor given as:

$$\beta_s = \frac{2y_c}{d} \tag{3}$$

where y_c is the distance from the elastic neutral axis to the extreme compression fiber and d is the overall depth of the member. For sections symmetrical about the axis of bending, β_s=1. For sections with first yield in tension, β_s<1 and the strength prediction increases. For sections with first yield in compression, β_s>1 and the strength prediction decreases.

Another factor influencing flexural strength for unsymmetric sections is the significant stress redistribution which occurs for open sections with the free edges in compression, such as tracks with unstiffened legs in compression or hat shapes with stiffened legs in compression. The section factor α_s is used to address these cases, where α_s =1 for most sections, and α_s=0 for sections like tracks and hats with free edges in compression where the strength drops more rapidly as slenderness increases. Note, consistent with DSM implementation in AISI S100 to date, Equation 1 includes local-global interaction, while Equation 2 ignores such interaction.

The factors k_s, β_s, and α_s can substantially alter the flexural strength curves as illustrated in Figure 1 for local buckling. The distortional buckling curves have similar variation.

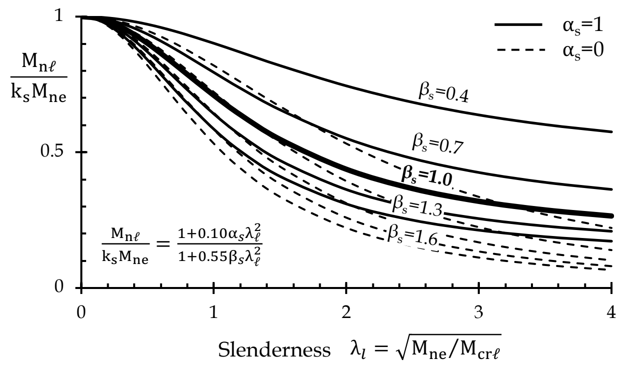

Figure 1: Local buckling flexural strength curves

Table 1 summarizes the performance of the proposed equations compared to the current DSM (AISI S100-16, [1]). The targeted data used to develop the proposed equations consisted entirely of unsymmetric sections with a wide range influencing factors. These equations where then checked against the legacy DSM data to confirm performance. The symmetric sections in the legacy data had little change (as intended), and the unsymmetric sections improved significantly. The new expressions handle unsymmetric sections with far greater accuracy, and provide one consistent and continuous strength expression from M_p to minimal capacity.

Table 1: Mean test-to-predicted ratios (CoV) for flexure

Data Used[a]	Symmetric	Mode[b]	Tests	S100-16	New DSM
Targeted	No	LB	216	1.32 (26%)	1.09 (7%)
Targeted	No	DB	283	1.02 (19%)	1.08 (15%)
Legacy	No	LB	69	1.15 (23%)	1.06 (10%)
Legacy	No	DB	140	1.12 (13%)	1.08 (13%)
Legacy	Yes	LB	147	1.01 (9%)	1.03 (9%)
Legacy	Yes	DB	232	1.07 (12%)	1.07 (12%)
Combined			1087	1.11 (18%)	1.07 (11%)
LRFD ϕ				0.88	0.93

[a] See Glauz and Schafer [8], [b] LB=Local Buckling, DB=Dist. Buckling

3 COMPRESSION MEMBERS

The current DSM strength curves for compression members do not require any of the adjustments made for flexural members. The factors k_s, β_s, and α_s are specific to the stress redistribution exhibited in flexure. For consistency and to simplify the strength prediction of beam-columns, the form of Equations 1 and 2 can be used for columns. The coefficients in Equations 4 and 5 were selected to match the current DSM strength predictions. The 1.2 pre-factor is added to establish the yield strength plateau at low slenderness as done with the current DSM curves, effectively shifting the curves upward.

$$P_{n\ell} = 1.2P_{ne}\frac{1+0.10\lambda_\ell^2}{1+0.55\lambda_\ell^2} \le P_{ne} \qquad \lambda_\ell^2 = \frac{P_{ne}}{P_{cr\ell}} \tag{4}$$

$$P_{nd} = 1.2P_y\frac{1+0.05\lambda_d^2}{1+0.67\lambda_d^2} \le P_y \qquad \lambda_d^2 = \frac{P_y}{P_{crd}} \tag{5}$$

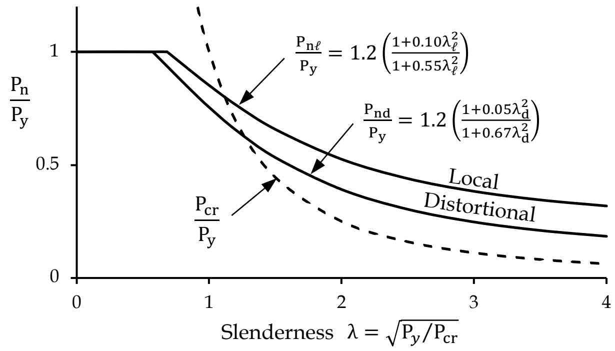

Figure 2: Column strength curves for local and distortional buckling

These equations are plotted in Figure 2 for the fully braced condition (P_{ne}=P_y). The strength predictions are very close to the current DSM. The local buckling equation aligns with the current DSM with a mean of 1.00 and CoV of 1.7% for $\lambda_\ell < 4$. The distortional buckling equation aligns with the current DSM with a mean of 1.00 and CoV of 1.2% for $\lambda_d < 4$. At higher slenderness, these proposed equations begin to deviate from the current DSM and little data exists to validate one or the other. Therefore, the strength predictions at high slenderness should be used with caution, see additional discussion in the summary.

4 MEMBERS WITH HOLES

The current DSM provisions for local and distortional buckling of members with holes were based on the research by Moen and Schafer [9,10,11]. Strength transition options were investigated where low slenderness was controlled by yielding of the net section and high slenderness was controlled by buckling using the current DSM strength curve. The proposed DSM equation form lends itself nicely to such a transition using a single equation. The following equations provide the net section strength at low slenderness with a smooth transition to the base curve without holes as slenderness increases, where the slenderness uses the elastic buckling force/moment considering the influence of the holes. The local buckling equations are plotted in Figures 3 and 4.

$$P_{n\ell} = 1.2P_{ynet}\frac{1+0.10\lambda_\ell^2}{1+0.55\lambda_\ell^2\left(\frac{P_{ynet}}{P_{ne}}\right)} \leq P_{ynet} \tag{6}$$

$$P_{nd} = 1.2P_{ynet}\frac{1+0.05\lambda_d^2}{1+0.67\lambda_d^2\left(\frac{P_{ynet}}{P_y}\right)} \leq P_{ynet} \tag{7}$$

$$M_{n\ell} = M_{pnet}\frac{1+0.10\alpha_s\lambda_\ell^2}{1+0.55\beta_s\lambda_\ell^2\left(\frac{M_{pnet}}{k_sM_{ne}}\right)} \tag{8}$$

$$M_{nd} = M_{pnet}\frac{1+0.07\lambda_d^2}{1+0.60\lambda_d^2\left(\frac{M_{pnet}}{M_p}\right)} \tag{9}$$

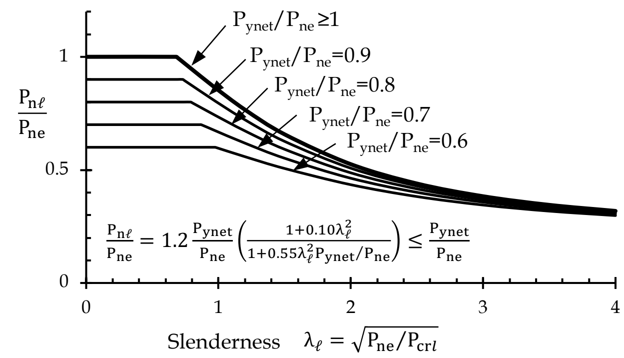

Figure 3: Local buckling column strength with holes

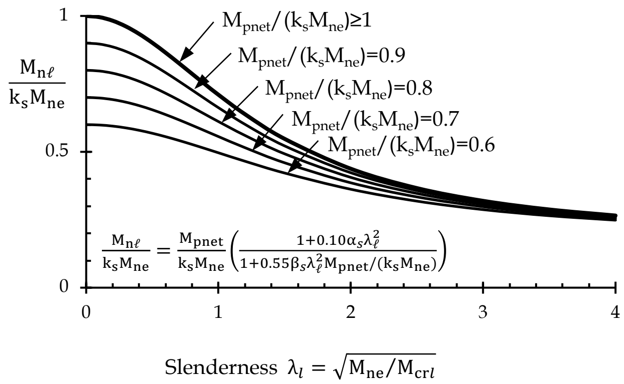

Figure 4: Local buckling flexural strength with holes

Equations 6-9 provide a lower CoV and better reliability than the current DSM equations as summarized in Table 2.

Table 2: Mean test-to-predicted ratios (CoV) for members with holes

Limit Sate	Equation	Tests	Mean (CoV)	LRFD ϕ
$P_{n\ell}$	6	195	1.07 (12%)	0.92
P_{nd}	7	265	1.11 (15%)	0.92
$M_{n\ell}$	8	81	1.07 (7%)	0.96
M_{nd}	9	165	1.09 (9%)	0.97

5 BEAM-COLUMNS

The DSM strength prediction for beam-columns was developed by Torabian and Schafer [12], where the DSM expressions for strength of beams and columns are merged to predict the strength of a member subject to both flexure and compression. The new form of local and distortional buckling strength equations for beams and columns permit a clean implementation for beam-columns, where the slenderness coefficients transition between the column values and beam values. These hybrid strengths are given by the following equations:

$$\beta_{n\ell} = k_\ell \beta_{ne} \frac{1+a_\ell\lambda_\ell^2}{1+b_\ell\lambda_\ell^2} \leq \beta_p \tag{10}$$

$$k_\ell = 1.2 + (k_s - 1.2)\gamma_\ell \tag{11}$$

$$a_\ell = 0.10 + (0.10\alpha_s - 0.10)\gamma_\ell \tag{12}$$

$$b_\ell = 0.55 + (0.55\beta_s - 0.55)\gamma_\ell \tag{13}$$

$$\beta_{nd} = k_d \beta_y \frac{1+a_d \lambda_d^2}{1+b_d \lambda_d^2} \leq \beta_p \quad (14)$$

$$k_d = 1.2 + (k_s - 1.2)\gamma_d \quad (15)$$

$$a_d = 0.05 + (0.07\alpha_s - 0.05)\gamma_d \quad (16)$$

$$b_d = 0.67 + (0.60\beta_s - 0.67)\gamma_d \quad (17)$$

The proportioning of the column and beam coefficients are managed by the transfer functions γ_ℓ and γ_d. Several forms of these functions were investigated, with the best fit being $\gamma_\ell = (1 - \cos\varphi_{PM})^4$ and $\gamma_d = (1 - \cos\varphi_{PM})^{10}$, where φ_{PM} is the angle of the load vector between compressive and flexural demands. The performance of these equations is summarized in Table 3.

Table 3: Mean test-to-predicted ratios (CoV) for beam-columns

Loading	Tests	Original[a]	New DSM
P+M_1	46	1.07 (12%)	1.08 (12%)
P+M_1+M_2	85	1.17 (17%)	1.14 (15%)
P+M_2	80	1.17 (19%)	1.15 (17%)
Combined	211	1.15 (17%)	1.13 (16%)
LRFD ϕ		0.88	0.89

[a] Beam-column provisions by Torabian and Schafer [12]

The predictions for compression and major axis bending (P+M_1) are essentially unchanged (as intended), whereas loadings containing M_2 are improved by use of the factors k_s, β_s, and α_s for the minor axis bending component.

6 SHEAR STRENGTH

The AISI [1] provisions for the shear strength of webs have been updated in Supplement 3 (published in 2022) based on the work by Pham, Pham, and Hancock [13]. The shear strength curves are given by Equation 18 for webs without transverse stiffeners and Equation 19 for webs with transverse web stiffeners.

$$V_n = \left[1 - 0.25\left(\frac{V_{cr}}{V_y}\right)^{0.65}\right]\left(\frac{V_{cr}}{V_y}\right)^{0.65} \mathrm{V_y} \ \text{ for } \lambda_v > 0.587 \quad (18)$$

$$V_n = \left[1 - 0.15\left(\frac{V_{cr}}{V_y}\right)^{0.4}\right]\left(\frac{V_{cr}}{V_y}\right)^{0.4} \mathrm{V_y} \ \text{ for } \lambda_v > 0.776 \quad (19)$$

The data used to develop and validate these AISI equations was fit to the new form of DSM equation, resulting in Equation 20 for webs without transverse stiffeners, and Equation 21 with transverse stiffeners. Performance of these equations are compared in Table 4 for webs with and without holes, where some improvement was achieved, particularly at higher slenderness.

$$V_n = \frac{1.2V_y}{1+0.57\lambda_v^2} \leq V_y \quad (20)$$

$$V_n = 1.2V_y \frac{1+0.05\lambda_v^2}{1+0.45\lambda_v^2} \leq V_y \quad (21)$$

Table 4: Mean test-to-predicted ratios (CoV) for shear

Transverse Web Stiff.	Web Holes	Tests	S100-16[a]	New DSM	LRFD ϕ
No	No	57	1.03 (8.9%)	1.00 (8.5%)	0.89
Yes	No	60	1.00 (6.6%)	1.00 (5.9%)	0.90
No	Yes	61	1.19 (17%)	1.17 (17%)	0.95
Yes	Yes	72	1.03 (6.3%)	1.04 (5.9%)	0.94

[a] S100-16 with Supplement 3

The strength curves for these proposed shear strength equations are plotted in Figure 5.

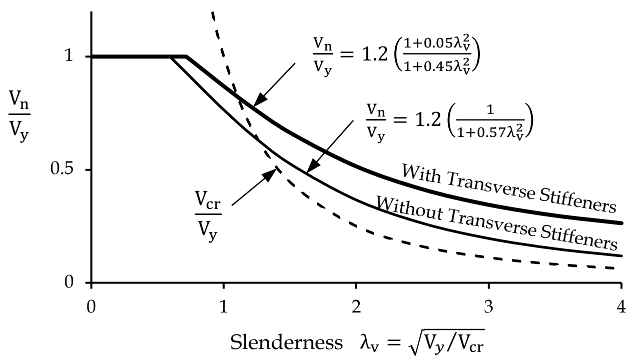

Figure 5: Shear strength with and without transverse stiffeners

7 SUMMARY AND DISCUSSION OF NEW DSM EXPRESSIONS

All of the strength equations presented herein using the proposed new form of DSM are concisely shown in Table 5. Also included are torsion bimoment strengths $B_{n\ell}$ and B_{nd} proposed in recent research by Xia et al. [14].

Table 5: DSM Equation Summary

$$\frac{R_n}{R_m} = \frac{1 + a\lambda^2}{1 + b\lambda^2}$$

R_n	R_m	λ^2	a	b
$P_{n\ell}$	$1.2P_{ne}$	$P_{ne}/P_{cr\ell}$	0.10	0.55
P_{nd}	$1.2P_y$	P_y/P_{crd}	0.05	0.67
$M_{n\ell}$	k_sM_{ne}	$M_{ne}/M_{cr\ell}$	$0.10\alpha_s$	$0.55\beta_s$
M_{nd}	M_p	M_y/M_{crd}	$0.07\alpha_s$	$0.60\beta_s$
$\beta_{n\ell}$	$(1.2\rightarrow k_s)\beta_{ne}$	$\beta_{ne}/\beta_{cr\ell}$	$0.10\rightarrow 0.10\alpha_s$	$0.55\rightarrow 0.55\beta_s$
β_{nd}	$(1.2\rightarrow k_s)\beta_y$	β_y/β_{crd}	$0.05\rightarrow 0.07\alpha_s$	$0.67\rightarrow 0.60\beta_s$
V_n	$1.2V_y$	V_y/V_{cr}	0	0.57
V_n^*	$1.2V_y$	V_y/V_{cr}	0.05	0.45
$B_{n\ell}$	B_p	$B_y/B_{cr\ell}$	0.094	0.23
B_{nd}	B_p	B_y/B_{crd}	0	1.11

* with transverse web stiffeners

The single equation provides the ratio of nominal strength R_n to maximum strength R_m using a simple slenderness expression with two coefficients, a and b. For compression and shear, the strength is capped at yield. For local and distortional buckling of members with holes, the maximum strength is based on yield of the net section, and the b coefficient is multiplied by $R_{m,net}/R_m$ to transition toward the gross section curve as slenderness increases.

As observed herein the new functional form for DSM provides several nice advantages when compared to the modified Winter format previously employed. At low slenderness the new form asymptotes to R_m and does not require the careful checking at a limiting lambda to avoid the nonlinear behavior as $\lambda \rightarrow 0$ in the modified Winter expression. For unsymmetric members in bending, as shown in [8], it is possible to modify the existing DSM expressions with β_s; however, the more drastic reductions implemented with α_s cannot be readily implemented – again demonstrating the flexibility with the new format.

DSM's origins can be understood as various forms of power law expressions (i.e., normalized strength$\cong \lambda^c$) as detailed in [15]. The new expression is different and does not asymptote to a power law in the same manner. However, if we take the slope of the new expression in log-log space we can find an estimate of the power law coefficient. The minimum power law coefficient may be shown to occur at λ_{min} with a coefficient as follows:

$$\lambda_{min} = 1/(a^{1/4} b^{1/4}) \tag{22}$$

$$c_{min} = (2a - 2b)/\left(\sqrt{a} + \sqrt{b}\right)^2 \tag{23}$$

The resulting minimum power law coefficients are compared to benchmarks and the previous DSM in Table 6. The comparison is another illustration of the wide range of strength predictions that are possible in the new format. Note, when a=0 the expressions default to the classic elastic buckling power law – in many cases the new expressions provide a different insight into the basic relationship with slenderness.

Table 6: Comparison to Power Law Expressions (λ^c)

R_n	λ^2	a	b	λ_{min}	c_{min}
Elastic	P_y/P_{cr}	N/A	N/A	N/A	-2
S100-16 P_{nd}	P_y/P_{crd}	N/A	N/A	N/A	-1.2
S100-16 P_{nl}	$P_{ne}/P_{cr\ell}$	N/A	N/A	N/A	-1
$P_{n\ell}$	$P_{ne}/P_{cr\ell}$	0.10	0.55	2.06	-0.80
P_{nd}	P_y/P_{crd}	0.05	0.67	2.34	-1.14
$M_{n\ell}$	$M_{ne}/M_{cr\ell}$	$0.10\alpha_s$	$0.55\beta_s$	2.46 -	-0.50 ($\alpha_s=1, \beta_s=0.5$) to -2 ($\alpha_s=0$)
M_{nd}	M_y/M_{crd}	$0.07\alpha_s$	$0.60\beta_s$	2.63 -	-0.70 to ($\alpha_s=1, \beta_s=0.5$) -2 ($\alpha_s=0$)
V_n	V_y/V_{cr}	0	0.57	-	-2
V_n^*	V_y/V_{cr}	0.05	0.45	2.58	-1.0
$B_{n\ell}$	$B_y/B_{cr\ell}$	0.094	0.23	2.61	-0.44
B_{nd}	B_y/B_{crd}	0	1.11	-	-2

* with transverse web stiffeners

Note, as $\lambda \rightarrow \infty$, R_n/R_m asymptotes to a/b. This implies a constant strength, which may be rational if a portion of the section (e.g. the corners) provides strength regardless of cross-section slenderness, but it is a divergence from past practice which converged to a power law (e.g. λ^{-1}). This difference in prediction as a function of slenderness begins at the minimum power coefficient location, λ_{min}, and becomes noticeable in most cases at $\lambda > 5$ (an exceedingly rare case in practice).

Not shown herein is the fact that the global buckling strength expressions may readily be fit into the same format. For practical reasons existing global strength expressions are being maintained in the AISI standard, but the beam-column expressions become further simplified if the global strength curves also utilize the new format.

Adoption of the new expressions is underway in the AISI standards. However, cold-formed steel standards development in the United States is moving to a new standards development organization – the end result is that it is not expected that the new expressions will be in the new standard and adopted until 2027; however, the authors are both fully engaged in the codes and standards development process and look forward to bringing the entire suite of expressions to the practicing engineering community in the near future.

8 CONCLUSIONS

The new form of DSM equation developed to handle the unique flexural strength requirements associated with members unsymmetric about the axis of bending has been successfully applied to local and distortional buckling of compression members, flexural and compression members with holes, beam-columns, shear strength with and without holes, and torsional bimoment strength. The benefits of this new form include: simpler expressions, single equation across all slenderness values, natural accommodation of flexural factors, ability to fit test data with better results, and clean support of strength transition for members with holes.

REFERENCES

[1] AISI S100-16, North American Specification for the Design of Cold-Formed Steel Structural Members. AISI, Washington, DC, 2016.

[2] AS/NZS 4600:2018, Cold-Formed Steel Structures. Standards Australia Limited, Standards New Zealand, 2018.

[3] Baur, S.W., and LaBoube, R.A., "Behavior of complex hat shape cold-formed steel members," Proceedings of Structural Stability Research Council, 2001.

[4] Nuttayasakul, N. and Easterling, W.S., "Cold-formed steel flexural members undergoing distortional and euler buckling," Proceedings of the Structural Stability Reseach Council, 2003.

[5] Oey, O. and Papangelis, J., "Behavior of cold-formed steel channels bent about the minor axis," Thin-Walled Structures 164, 2021.

[6] Raebel, C.H. and Gwozdz, D., "Experimental and Numerical Comparison of Flexural Capacity of Light Gage Cold Formed Steel Roof Deck," Milwaukee School of Engineering Report No. MSOE-CAECM-CVE-17-10, 2017.

[7] Degtyarev, V.V., "Computational study of elastic buckling and post-buckling strength of steel decks in bending," Proceedings of the Annual Stability Conference, SSRC, 2020.

[8] Glauz, R.S. and Schafer, B.W., "Modifications to the Direct Strength Method of cold-formed steel design for members unsymmetric about the axis of bending," Thin-Walled Structures 173, 2022.

[9] Moen, C.D. and Schafer, B.W., "Direct Strength Design of Cold-Formed Steel Members with Perforations," AISI Research Report RP09-1, March 2009.

[10] Moen, C.D. and Schafer, B.W., "Direct Strength Design of Cold-Formed Steel Columns with Holes," Proceedings of the Annual Stability Conference, SSRC, 2010.

[11] Moen, C.D. and Schafer, B.W., "Extending Direct Strength Design to Cold-Formed Steel Beams with Holes," Proceedings of the International Specialty Conference on Cold-Formed Steel Structures, 2010.

[12] Torabian, S. and Schafer, B.W., "Development and Experimental Validation of the Direct Strength Method for Cold-Formed Steel Beam-Columns," ASCE Journal of Structural Engineering 144(10), 2018.

[13] Pham, S.H., Pham, C.H., and Hancock, G.J., "New Proposal for the Shear Strength of Unstiffened Cold-Formed Steel Beam Webs," Proceedings of the Cold-Formed Steel Research Consortium Colloquium, 2020.

[14] Xia, Y., Glauz, R.S., Schafer, B.W., Seek, M.W., Blum, H.B., "Cold-formed steel strength predictions for torsion" Proceedings of the Annual Stability Conference, SSRC, 2022.

[15] Schafer, B.W., "Advances in the Direct Strength Method of cold-formed steel design," Thin-walled Structures, 140, 533-541, 2019.